Journal of
# Mechanics of
# Materials and Structures

## INTERFACE STRESS OF ORTHOTROPIC MATERIALS WITH A NANODEFECT UNDER ANTIPLANE SHEAR LOADING

Junhua Xiao, Chuanfu Shi, Yaoling Xu and Fucheng Zhang

Volume 11, No. 5 December 2016

msp

JOURNAL OF MECHANICS OF MATERIALS AND STRUCTURES
Vol. 11, No. 5, 2016
dx.doi.org/10.2140/jomms.2016.11.491

# INTERFACE STRESS OF ORTHOTROPIC MATERIALS WITH A NANODEFECT UNDER ANTIPLANE SHEAR LOADING

JUNHUA XIAO, CHUANFU SHI, YAOLING XU AND FUCHENG ZHANG

A theoretical study is conducted on an orthotropic solid with a nanodefect (e.g., inclusion, hole, or crack) under far-field antiplane shear loading. A rigorous analytical solution of the stress fields is presented using the Gurtin–Murdoch surface/interface model and a conformal mapping technique. Several new and existing solutions are considered for the special and degenerated cases. The major results of the study are as follows:

(1) Interface stresses are greatly dependent on size when the size of a defect is at the nanometer scale, and the interface stresses approach the classical elasticity results when a defect has large characteristic dimensions.
(2) The interface effect of a nanodefect decreases with an increase in defect section aspect ratio.
(3) When the modulus of the defect (inclusion) increases, the interface effect decreases, i.e., the interface effect can be neglected when the inclusion is sufficiently hard.

## 1. Introduction

Several composite materials can be regarded as orthotropic solids in engineering applications. The general properties, as well as the fracture and damage properties, of orthotropic solids have received considerable attention with respect to elastic-plastic and fracture damage theories. When the size of defects (e.g., inclusion, hole, or crack) in an orthotropic solid is at the nanometer scale, the interface effect of nanodefects plays an important role in micromechanical properties because of the high surface-to-volume ratios of this solid material [Nan and Wang 2013; Grekov and Yazovskaya 2014].

In recent years, significant progress has been made in addressing the fracture characteristics of orthotropic solids with holes or cracks from a fundamental perspective by applying classical elastoplastic theory. Tang and Hwang [1991] discussed the near-tip field solution for a plane stress mode I stationary crack in an elastic-perfectly orthotropic plastic material based on phenomenological plasticity theory. Gao and Tong [1995] used the Cauchy integral method to study the fundamental solutions for the complex stress functions and the stress intensity factors of an equal-parameter orthotropic plate with an elliptical hole or crack. Ozturk and Erdogan [1997] formulated the mode I crack problem for an inhomogeneous orthotropic plane and obtained a solution for various loading conditions and material parameters. Kim, Lee, and Joo [1999] presented a numerical solution by applying the Fourier integral transform method on the problem of a three-layered orthotropic material with a center crack that was subjected to an arbitrary antiplane shear loading. Berbinau and Soutis [2001] presented a new analytical method for solving mixed boundary value problems along holes in orthotropic plates. Kwon and Meguid [2002] proposed a general solution for the field intensity factors and the energy release rate of a Griffith crack normal to

*Keywords:* orthotropic materials, nanodefects, interface stresses, antiplane shear, Gurtin–Murdoch surface/interface model.

the interface between a rectangular piezoelectric ceramic and two of the same rectangular orthotropic materials with finite lengths under combined in-plane electrical and antiplane mechanical loadings. Lee, Kwon, Lee, and Kwon [2002] provided the dynamic field intensity factors for the problem of an interfacial crack moving along the interface between a piezoelectric material and two orthotropic materials under electromechanical longitudinal shear loading. Li [2003] analytically determined the stress intensity factors for the problem of an orthotropic strip with two collinear cracks normal to the strip boundaries under remote uniform antiplane shear loading. Faal and Fariborz [2007] derived the stress fields in an orthotropic infinite plane with Volterra-type climb and glide edge dislocations. Chalivendra [2008] developed quasistatic stress fields for a crack oriented along one of the principal axes of an inhomogeneous orthotropic medium by conducting asymptotic analysis coupled with the Westergaard stress function approach. Zhang and Deng [2008] derived elastic stress fields near the cohesive zone of a crack aligned with the principal axes of a degenerated orthotropic material using complex variable and eigenfunction expansion methods. Xiao and Jiang [2009] obtained a closed-form solution for orthotropic materials weakened by a doubly periodic array of cracks under far-field antiplane shear loading by applying elliptical function and analytical function theories on the boundary value problems. Moharrami and Ayatollahi [2011] conducted stress analysis on an orthotropic plane with a Volterra-type dislocation. The distributed dislocation technique was adopted to obtain the integral equations for an orthotropic plane weakened by cracks under time-harmonic antiplane traction. Goldstein and Shifrin [2012] investigated a crack that was initially located on a symmetry axis of an orthotropic plane and subjected to biaxial loading. Liu and Zhou [2014] presented a solution for a plane rectangular crack in a 3D infinite orthotropic elastic material by applying a generalization of Almansi's theorem and the Schmidt method. Liu, Zhou, Wu, and Wu [2015] investigated a nonlocal theory solution for a rectangular crack in a 3D infinite orthotropic elastic medium using a generalization of Almansi's theorem and the Schmidt method. Peng, Li, and Feng [2015] investigated the interaction between a mode I crack and a symmetrical shape inclusion in an orthotropic medium subjected to remote stress by using transformation toughening theory and the Eshelby inclusion method.

Extensive investigations have also been conducted on the effective properties of orthotropic composite solids. Zhao and Yu [2000] presented a model for orthotropic damage on materials by combining the macroscopic mechanical properties with the microstructure parameters of a material based on Eshelby's equivalence principle. Bouyge, Jasiuk, Boccara, and Ostoja-Starzewski [2002] determined the couple-stress moduli and characteristic lengths of a 2D matrix-inclusion composite with the inclusions arranged in a periodic square array and both linear elastic constituents being of Cauchy type. Yang and Becker [2004] studied the effective properties and microscopic deformation of anisotropic plates with periodic holes via direct mathematical homogenization. Ieşan and Scalia [2007] investigated linear theory of inhomogeneous and orthotropic elastic materials with voids. Nie, Chan, Shin, and Roy [2008] presented analytic solutions for elastic fields induced by normal and shear eigenstrains in an elliptical region embedded into orthotropic composite materials by applying conformal transformation and the complex function method. Monchiet, Gruescu, Cazacu, and Kondo [2012] achieved effective compliance of an orthotropic medium with arbitrarily oriented cracks by using newly derived expressions of the Eshelby tensor.

The present work constitutes research on the interface stresses of an orthotropic solid with a nanodefect. A closed-form solution for the problem of orthotropic materials with a nanosized elliptical defect is presented under antiplane shear loading by applying the Gurtin–Murdoch surface/interface model and a conformal mapping technique. The influences of defect size, matrix material moduli ratio, defect shape ratio, and defect elastic property on stress fields are discussed.

## 2. Computational model and basic equations

A schematic diagram of an orthotropic solid with an isotropic nanodefect (i.e., nanoelliptical inclusion) that considers the interface effect is presented in Figure 1. Regions $\Omega_{\mathrm{I}}$ and $\Omega_{\mathrm{M}}$ denote the elliptical defect and the matrix, respectively. The Gurtin–Murdoch surface/interface model [Gurtin and Murdoch 1975; 1978; Gurtin et al. 1998] indicates that interface $L$ can be regarded as a layer without thickness and with different material properties from the defect and the matrix. The semimajor and semiminor axes of the elliptical defect are denoted as $a$ and $b$, respectively. I, 0, and M denote the defect, interface, and matrix, respectively. $G_{\mathrm{I}}$ denotes the antiplane shear modulus of the defect (inclusion). $C_{44}$ and $C_{55}$ are the principal shear moduli of the orthotropic solid, which are located along the $y$- and $x$-axes in Figure 1, respectively. The $Oz$-axis is perpendicular to the section in the Cartesian coordinate system. The matrix is subjected to far-field antiplane shear stress $\tau_{yz}^{\infty}$.

The governing equation and the constitutive equation of the matrix can be given as [Li 2003]

$$\frac{\partial \tau_{xz}}{\partial x} + \frac{\partial \tau_{yz}}{\partial y} = 0, \tag{1}$$

$$\begin{Bmatrix} \tau_{xz} \\ \tau_{yz} \end{Bmatrix} = \begin{bmatrix} C_{55} & 0 \\ 0 & C_{44} \end{bmatrix} \begin{Bmatrix} \partial w/\partial x \\ \partial w/\partial y \end{Bmatrix}, \tag{2}$$

where $w$ is the antiplane displacement.

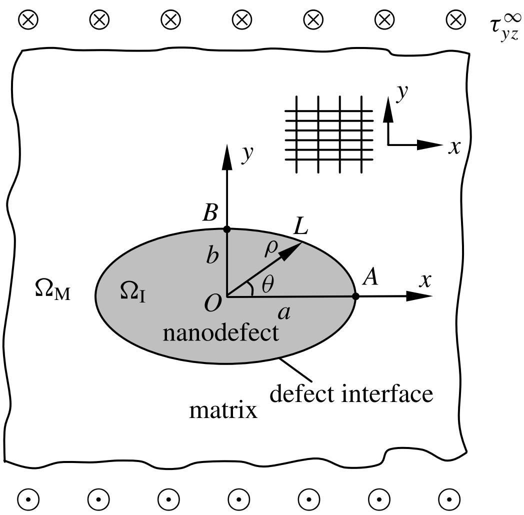


**Figure 1.** Schematic diagram of an orthotropic solid with an nanodefect (nanoelliptic inclusion) considering interface effect ($z$-plane, $z = x + \mathrm{i}y$).

Nonclassical boundary conditions on nanodefect interface $L$ can be written as [Luo and Wang 2009; Sharma et al. 2003]

$$w_{\mathrm{P}}(t) = w_{\mathrm{M}}(t) \qquad t = \rho e^{\mathrm{i}\theta}, \tag{3}$$

$$\tau_{rz}^{\mathrm{P}}(t) - \tau_{rz}^{\mathrm{M}}(t) = \frac{2\mu^S}{\rho}\frac{\partial \epsilon_{\theta z}^0}{\partial \theta} \quad t = \rho e^{\mathrm{i}\theta}, \tag{4}$$

where $(\rho, \theta)$ denotes the polar coordinates on the interface $L$; $\tau_{\theta z}^0$ and $\epsilon_{\theta z}^0$ denote the stress and strain components on the interface, respectively; $\mu^S = C_{44}^S|\sin\theta| + C_{55}^S|\cos\theta|$; and $C_{44}^S$ and $C_{55}^S$ denote the interface elastic constants along the $y$- and $x$-axes in Figure 1, respectively. The unit for interface elastic constants $C_{44}^S$ and $C_{55}^S$ is N/m. The expression of $\mu^S$ in terms of $\theta$ is merely an assumption made by the authors.

The interfacial strain for a coherent interface is equal to the associated tangential strain in the abutting materials, i.e.,

$$\epsilon_{\theta z}^0 = \epsilon_{\theta z}^{\mathrm{P}} = \epsilon_{\theta z}^{\mathrm{M}}. \tag{5}$$

## 3. Analysis and solution

By substituting (2) into (1), a second-order linear homogeneous partial differential equation with constant coefficients on $w$ is obtained as

$$C_{55}\frac{\partial^2 w}{\partial x^2} + C_{44}\frac{\partial^2 w}{\partial y^2} = 0. \tag{6}$$

The solution for (6) can be expressed as

$$w = \mathrm{Re}F(z_m), \tag{7}$$

where $f(z_m)$ is an analytical function with respect to $z_m$, $z_m = x + \mathrm{i}my$, and $m = \sqrt{C_{55}/C_{44}}$.

By substituting (7) into (2), the expressions obtained are

$$\begin{aligned} \tau_{xz} &= C_{55}\frac{\partial \mathrm{Re} f(z_m)}{\partial x} = C_{55}\mathrm{Re} f'(z_m), \\ \tau_{yz} &= mC_{44}\frac{\partial \mathrm{Re} f(z_m)}{\partial (my)} = -mC_{44}\mathrm{Im} f'(z_m), \end{aligned} \tag{8}$$

where $f'(z_m)$ denotes the derivative with respect to $z_m$. Then, (8) can be rewritten as

$$\frac{\tau_{xz}}{C_{55}} - \mathrm{i}\frac{\tau_{yz}}{\sqrt{C_{44}C_{55}}} = \mathrm{Re} f'(z_m) + \mathrm{i}\mathrm{Im} f'(z_m) = f'(z_m). \tag{9}$$

The $z_m$-plane (Figure 2) is generated by the map of $z_m = x + \mathrm{i}my$ from the $z$-plane (Figure 1), where $O_1$ and $O_2$ denote the foci of the elliptical inclusion.

To solve the problem in Figure 2, a new variable $\zeta$ is introduced as

$$\zeta = \xi + \mathrm{i}\eta = l e^{\mathrm{i}\phi}, \tag{10}$$

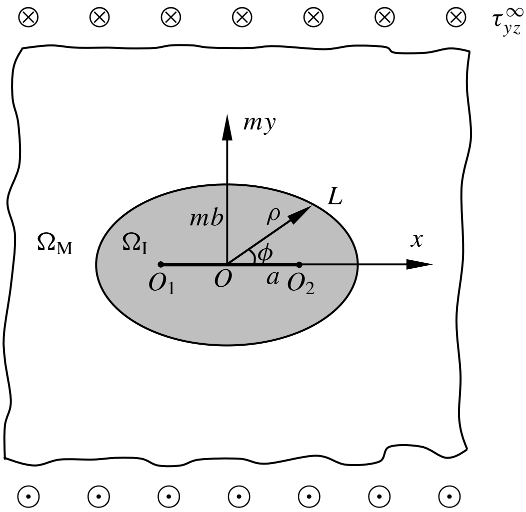


**Figure 2.** $z_m$-plane corresponding to the plane $z$ ($z_m = x + \mathrm{i}my$).

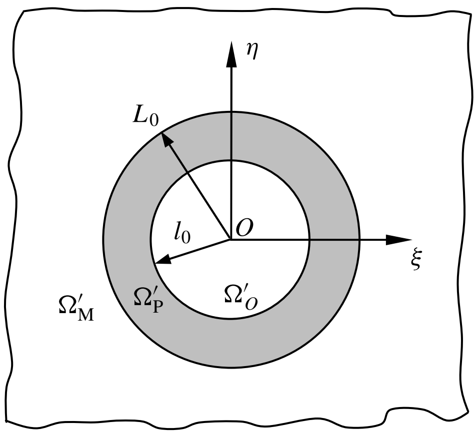


**Figure 3.** Conformal mapping in the $\zeta$-plane ($\zeta = \xi + \mathrm{i}\eta$).

where $(l, \phi)$ denotes the polar coordinates in the $\zeta$-plane. The $z_m$-plane is mapped onto the $\zeta$-plane via conformal transformation,

$$z_m = \Omega(\zeta) = \zeta + \frac{n}{\zeta}, \tag{11}$$

where $n = (a^2 - m^2 b^2)/4$. Region $\Omega_I$ in the $z_m$-plane is mapped onto circular region $\Omega'_O$, with radius $l_0$, and circular region $\Omega'_P$, with radius $L_0$, shown in Figure 3, respectively.

From the transformation relationship between Figures 2 and 3, the equations obtained are

$$x = \xi + \frac{n\xi}{\xi^2+\eta^2}, \quad my = \eta - \frac{n\eta}{\xi^2+\eta^2}. \tag{12}$$

From (12), the following expressions are derived:

$$l_0 = \sqrt{n}, \tag{13}$$

$$L_0 = \frac{a+mb}{2}. \tag{14}$$

In an annular region, an analytical function $F(\zeta)$ can be expanded into a Laurent series [Muskhelishvili 1953]:

$$F(\zeta) = a^* \ln \zeta + \sum_{k=-\infty}^{\infty} a_k \zeta^k, \tag{15}$$

where $a^*$ and $a_k$ are complex constants to be determined. The exact solution can be obtained by taking the following finite terms of the series:

$$F_{\mathrm{I}}(\zeta) = A_1\Big(\zeta + n/\zeta\Big) = A_1\Big(le^{\mathrm{i}\phi} + \frac{ne^{-\mathrm{i}\phi}}{l}\Big) \quad \text{in } \Omega_{\mathrm{I}}', \tag{16}$$

$$F_{\mathrm{M}}(\zeta) = B_1\zeta + B_{-1}\frac{1}{\zeta} \ = B_1 le^{\mathrm{i}\phi} + \frac{B_{-1}}{l}e^{-\mathrm{i}\phi} \quad \text{in } \Omega_{\mathrm{M}}', \tag{17}$$

where $A_1$, $B_1$, and $B_{-1}$ are complex constants.

By applying far-field conditions, coefficient $B_1$ can be obtained from (9) and (17) as

$$B_1 = -\mathrm{i}\frac{\tau_{yz}^{\infty}}{\sqrt{C_{44}C_{55}}}. \tag{18}$$

The boundary conditions on $L_0$ in Figure 3 can be summarized as

$$w_{\mathrm{I}}(z) = w_{\mathrm{M}}(z), \tag{19}$$

$$\tau_{rz}^{\mathrm{I}}(z) - \tau_{rz}^{\mathrm{M}}(z) = \frac{2\mu^S}{L_0}\frac{\partial \epsilon_{\theta z}^{L_0}}{\partial \theta}, \tag{20}$$

where $\mu^S = C_{44}^S|\sin\theta| + C_{55}^S|\cos\theta|$, and $C_{44}^S$ and $C_{55}^S$ denote the interface elastic constants along the $y$- and $x$-axes in Figure 1, respectively.

From boundary conditions (19) and (20), the expressions obtained are

$$\Big(1 + \frac{n}{L_0^2}\Big)A_1 = B_1 - \frac{B_{-1}}{L_0^2}, \tag{21}$$

$$\Big[G_{\mathrm{I}}\Big(1 - \frac{n}{L_0^2}\Big) + \frac{\mu^S}{L_0}\Big(1 + \frac{n}{L_0^2}\Big)\Big]A_1 = C_{44}\Big(B_1 + \frac{B_{-1}}{L_0^2}\Big). \tag{22}$$

By integrating (21) and (22) into (18), the expressions

$$A_1 = S_1 B_1, \quad B_{-1} = S_{-1}B_1, \tag{23}$$

are derived, where

$$S_1 = \frac{2C_{44}}{G_{\mathrm{I}}(1-n/L_0^2)+(\mu^S/L_0)(1+n/L_0^2)+C_{44}(1+n/L_0^2)},$$
$$S_{-1} = \frac{G_{\mathrm{I}}(1-n/L_0^2)+(\mu^S/L_0)(1+n/L_0^2)-C_{44}(1+n/L_0^2)}{G_{\mathrm{I}}(1-n/L_0^2)+(\mu^S/L_0)(1+n/L_0^2)+C_{44}(1+n/L_0^2)}L_0^2. \tag{24}$$

From (9), (16), (17), (18), and (23), the overall stress fields in the composites can be expressed as

$$\tau_{yz}+\mathrm{i}\tau_{xz} = G_{\mathrm{I}}S_1\frac{\tau_{yz}^{\infty}}{\sqrt{C_{44}C_{55}}} \quad \text{in the inclusion,} \tag{25}$$

$$\frac{\tau_{yz}}{\sqrt{C_{44}C_{55}}}+\mathrm{i}\frac{\tau_{xz}}{C_{55}} = \frac{\zeta^2-S_{-1}}{\zeta^2-n}\frac{\tau_{yz}^{\infty}}{\sqrt{C_{44}C_{55}}} \quad \text{in the matrix,} \tag{26}$$

where $\zeta=\xi+\mathrm{i}\eta=(z_m+\sqrt{z_m^2-4n})/2$, $z_m=x+\mathrm{i}my$.

## 4. Special cases

(1) *Orthotropic solid with a rigid nanoelliptical inclusion*:

Let $G_{\mathrm{I}}\to\infty$ in (25) and (26). The stress fields degenerate into

$$\tau_{yz}+\mathrm{i}\tau_{xz} = \frac{2C_{44}}{1-n/L_0^2}\frac{\tau_{yz}^{\infty}}{\sqrt{C_{44}C_{55}}} \quad \text{in the inclusion,} \tag{27}$$

$$\frac{\tau_{yz}}{\sqrt{C_{44}C_{55}}}+\mathrm{i}\frac{\tau_{xz}}{C_{55}} = \frac{\zeta^2-L_0^2}{\zeta^2-n}\frac{\tau_{yz}^{\infty}}{\sqrt{C_{44}C_{55}}} \quad \text{in the matrix.} \tag{28}$$

(2) *Orthotropic solid with a nanoelliptical hole*:

Let $G_{\mathrm{I}}=0$. Equation (26) degenerates into

$$\frac{\tau_{yz}}{\sqrt{C_{44}C_{55}}}+\mathrm{i}\frac{\tau_{xz}}{C_{55}} = \frac{\zeta^2-(\mu^S/L_0-C_{44})/(\mu^S/L_0+C_{44})L_0^2}{\zeta^2-n}\frac{\tau_{yz}^{\infty}}{\sqrt{C_{44}C_{55}}}. \tag{29}$$

Equation (29) agrees with the existing results [Xiao et al. 2014, Equation (23)].

(3) *Nanocrack in an orthotropic solid*:

Take $b=0$ in (29). The crack tip stress field can be obtained as

$$\frac{\tau_{yz}}{\sqrt{C_{44}C_{55}}}+\mathrm{i}\frac{\tau_{xz}}{C_{55}} = \frac{4\zeta^2-(2\mu^S/a-C_{44})/(2\mu^S/a+C_{44})a^2}{4\zeta^2-a^2}\frac{\tau_{yz}^{\infty}}{\sqrt{C_{44}C_{55}}}. \tag{30}$$

The III-type stress intensity factor at tip $A$ in Figure 1 can be defined as

$$K_{\mathrm{III}}^A = \lim_{\substack{y=0\\ z\to a}}\tau_{yz}\sqrt{2\pi(z-a)} = \tau_{yz}^{\infty}\sqrt{\pi a}\frac{C_{44}}{C_{44}+2\mu^s/a} = K_A^*\tau_{yz}^{\infty}\sqrt{\pi a}, \tag{31}$$

where $K_A^*=K_{\mathrm{III}}^A/(\tau_{yz}^{\infty}\sqrt{\pi a})$ denotes the dimensionless stress intensity factor at tip $A$. When ignoring the interface effect of inclusion, i.e., $\mu^s=0$, (31) degenerates into the existing solution presented by Hwu [1991], i.e.,

$$K_{\mathrm{III}}^A = \tau_{yz}^{\infty}\sqrt{\pi a}. \tag{32}$$

## 5. Results and discussion

The interface elastic constant can be obtained through atomistic simulations. Studies on orthotropic solids remain lacking; thus, we consider $C_{44}^S/C_{55}^S = C_{44}/C_{55}$ in this work. We assume that the ratio of the elastic constant $C_{44}^S$ of the interface to that of the matrix along the $y$-axis is a real constant $\alpha$, i.e., $\alpha = C_{44}^S/C_{44}$, where $\alpha$ varies from $-2\cdot 10^{-10}$ m to $2\cdot 10^{-10}$ m [Luo and Wang 2009]. Then, $\mu^S = C_{44}^S|\sin\theta| + C_{55}^S|\cos\theta| = C_{44}^S(|\sin\theta| + C_{55}/C_{44}|\cos\theta|)$. We then define the section aspect ratio of the elliptical inclusion as $\gamma = b/a$, $\beta = G_{\mathrm{I}}/C_{44}$.

**Example 1.** A comparison of the present solution for $\alpha = 0$ (classical elasticity theory) with the finite element results is plotted in Figure 4, where $a = 5$ nm, $\gamma = b/a = 0.5$, $\beta = G_{\mathrm{I}}/C_{44} = 0$, $C_{55} = 12$ GPa, and $C_{44} = 5.7$ GPa. The finite element results agree with the present solution when $\alpha = 0$. With the increase in angle $\theta$ from 0° to 90°, the interface stress concentration factors decrease monotonously when $\alpha = 2\cdot 10^{-10}$ m and $\alpha = 0$, whereas the interface stress concentration factors initially decrease and then increase when $\alpha = -2\cdot 10^{-10}$ m.

**Example 2.** The variation in the stress concentration factors at points $A$ and $B$ (Figure 1) with the semimajor axis of the inclusion is plotted in Figure 5, where $\gamma = b/a = 0.2$, $\beta = G_{\mathrm{I}}/C_{44} = 2$, and $C_{55}/C_{44} = 2$. Stress $\tau_{yz}^A$ is calculated using (26) when $\rho = a$ and $\theta = 0°$ (Figure 1). Then, stress $\tau_{yz}^A$ is the bulk stress, and stress concentration factor $\tau_{yz}^A/\tau_{yz}^\infty$ is dimensionless.

Figure 5 shows that stress concentration factors are dramatically dependent on size when the size of an elliptical inclusion is at the nanometer scale. The present solution approaches classical elasticity theory when the inclusion has large characteristic dimensions.

**Example 3.** The material moduli ratio $C_{55}/C_{44}$ can be regarded as a parameter in studying the influence of material orthotropy on stress concentration factors. The variation in the stress concentration factors

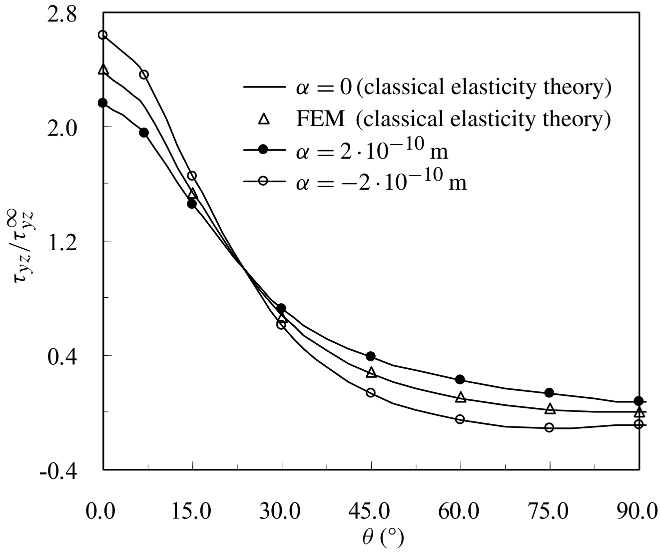


**Figure 4.** Distribution of the interface stress concentration factors on the interface of the elliptic hole.

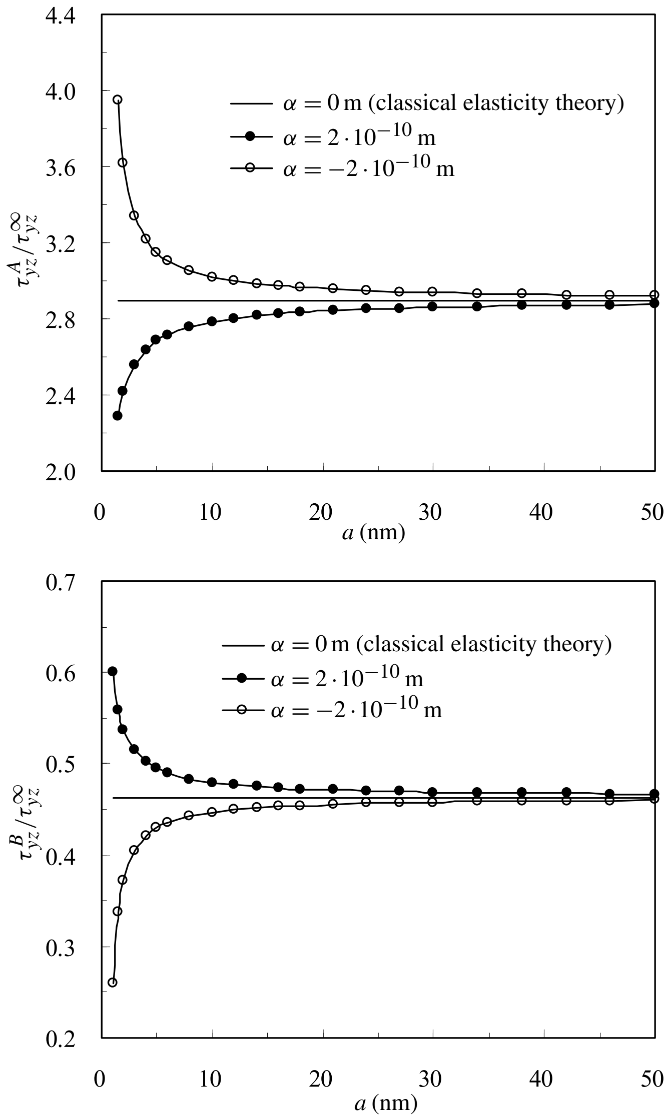


**Figure 5.** Variation of the stress concentration factors at points $A$ (top) and $B$ (bottom) with the size of the elliptic inclusion.

at points $A$ and $B$ with $\lg(C_{55}/C_{44})$ is plotted in Figure 6, where $a = 5\,\text{nm}$, $\gamma = b/a = 0.2$, and $\beta = G_{\text{I}}/C_{44} = 2$.

When the ratio of the elastic main direction $\lg(C_{55}/C_{44})$ increases, the increase in $C_{55}/C_{44}$ shields the stress concentration factor at point $A$ but amplifies said factor at point $B$.

**Example 4.** Figure 7 shows the variation in the stress concentration factors at points $A$ and $B$ with the inclusion section aspect ratio $\gamma = b/a$, where $a = 5\,\text{nm}$, $\beta = G_{\text{I}}/C_{44} = 2$, and $C_{55}/C_{44} = 2$.

When the inclusion section aspect ratio $\gamma$ increases gradually from 0 to 1, the stress concentration factor at point $A$ decreases monotonically, whereas at point $B$ it increases monotonically. The interface

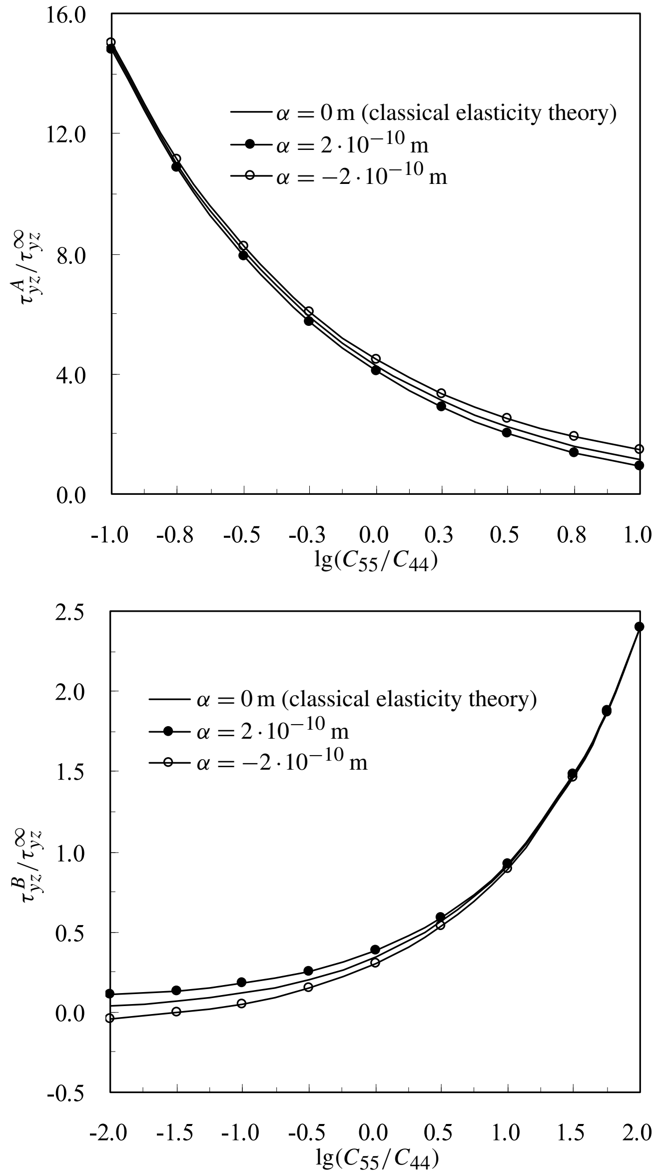


**Figure 6.** Variation of the stress concentration factors at points $A$ (top) and $B$ (bottom) with the ratio of the elastic main direction $C_{55}/C_{44}$.

effect of the nanoinclusion decreases with the increase in the inclusion section aspect ratio $\gamma$.

**Example 5.** The variation in the stress concentration factors at points $A$ and $B$ with the dimensionless logarithmic inclusion shear modulus $\lg(G_I/G_{44})$ is plotted in Figure 8, where $a = 5$ nm, $\gamma = b/a = 0.2$, and $C_{55}/C_{44} = 2$.

Figure 8 illustrates an interesting phenomenon in which the interface effect can be neglected when

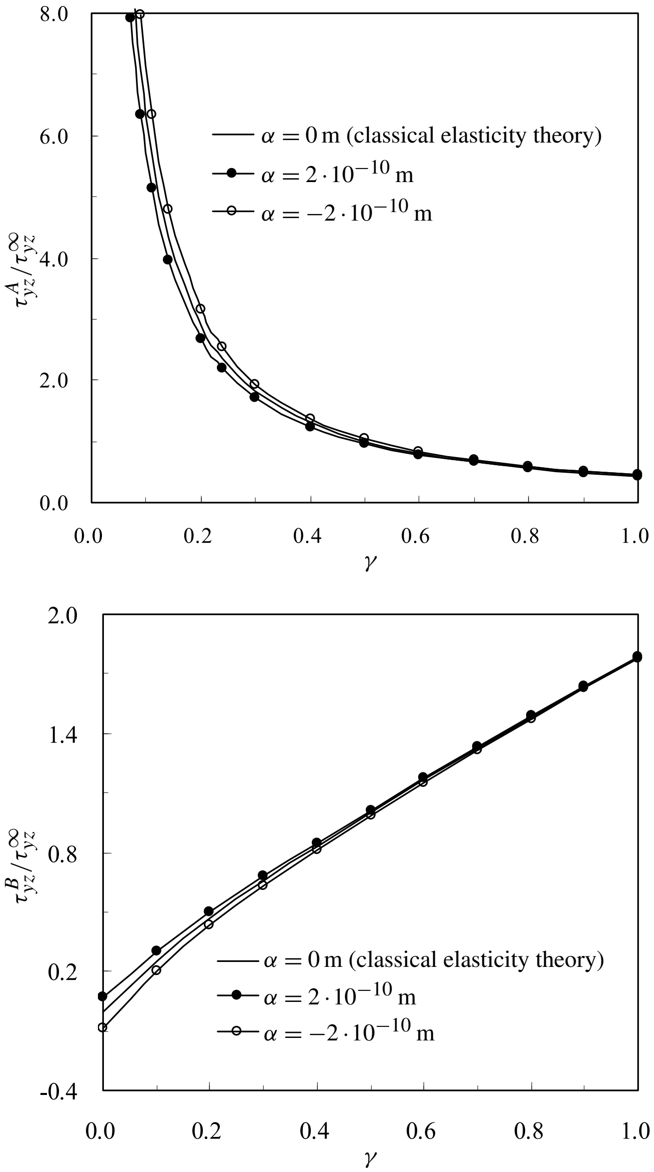


**Figure 7.** Variation of the stress concentration factors at points $A$ (top) and $B$ (bottom) with the elliptic inclusion shape ratio $\gamma = b/a$.

the inclusion is sufficiently hard. The influence of the interface effect depends on the modulus of the inclusion, i.e., the interface effect decreases with the increase in the modulus of the inclusion.

## 6. Conclusions

The problem of an orthotropic solid with a nanodefect under far-field antiplane shear loading was investigated using the Gurtin–Murdoch surface/interface model and a conformal mapping technique. An

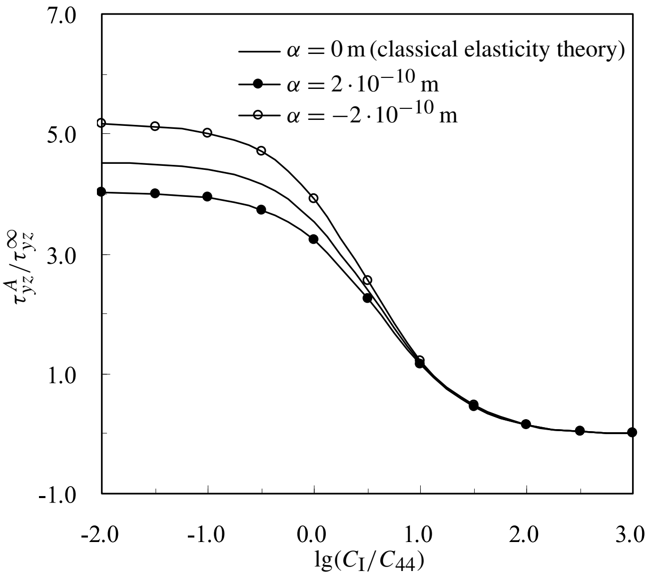


(a) Stress concentration factor at point $A$.

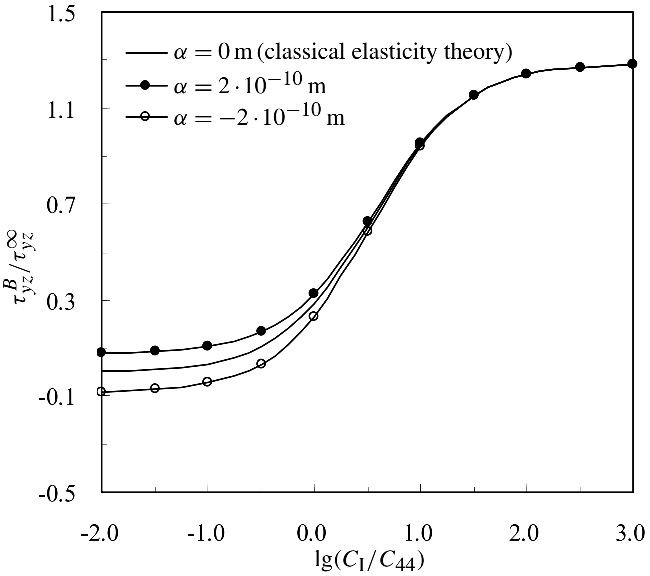


(b) Stress concentration factor at point $B$.

**Figure 8.** Variation of the stress concentration factors at points $A$ and $B$ with the elliptic cavity shape ratio $\gamma = b/a$.

analytical solution for the overall stress field in the nanoinhomogeneous material was obtained. The proposed solution is generalized, such that several new and existing solutions can be regarded as special or degenerate cases. The effects of defect size, matrix material moduli ratio, defect shape ratio, and inclusion elastic property on the interface stresses were discussed.

## Acknowledgments

This work was supported by the National Natural Science Foundation of China (11302186), the National Natural Science Foundation for Distinguished Young Scholars (50925522), the Hebei Province High School Top Young Talent (BJ2014058) and the Natural Science Foundation of Hebei Province (A2013203103, A2013203213).

## References

[Berbinau and Soutis 2001] P. Berbinau and C. Soutis, "A new approach for solving mixed boundary value problems along holes in orthotropic plates", *Int. J. Solids Struct.* **38**:1 (2001), 143–159.

[Bouyge et al. 2002] F. Bouyge, I. Jasiuk, S. Boccara, and M. Ostoja-Starzewski, "A micromechanically based couple-stress model of an elastic orthotropic two-phase composite", *Eur. J. Mech. A Solids* **21**:3 (2002), 465–481.

[Chalivendra 2008] V. B. Chalivendra, "Mode-I crack-tip stress fields for inhomogeneous orthotropic medium", *Mech. Mater.* **40**:4–5 (2008), 293–301.

[Faal and Fariborz 2007] R. T. Faal and S. J. Fariborz, "Stress analysis of orthotropic planes weakened by cracks", *Appl. Math. Model.* **31**:6 (2007), 1133–1148.

[Gao and Tong 1995] C. F. Gao and X. H. Tong, "The fundamental solutions for the equal-parameter orthotropic plate containing an elliptical hole or a crack", *Acta Mech. Sinica* **27**:5 (1995), 609–613. In Chinese.

[Goldstein and Shifrin 2012] R. V. Goldstein and E. I. Shifrin, "Conditions for Mode I crack deviation in orthotropic plane subjected to biaxial loading", *Int. J. Eng. Sci.* **61** (2012), 36–47.

[Grekov and Yazovskaya 2014] M. A. Grekov and A. A. Yazovskaya, "The effect of surface elasticity and residual surface stress in an elastic body with an elliptic nanohole", *J. Appl. Math. Mech.* **78**:2 (2014), 172–180.

[Gurtin and Murdoch 1975] M. E. Gurtin and A. I. Murdoch, "A continuum theory of elastic material surfaces", *Arch. Ration. Mech. Anal.* **57**:4 (1975), 291–323.

[Gurtin and Murdoch 1978] M. E. Gurtin and A. I. Murdoch, "Surface stress in solids", *Int. J. Solids Struct.* **14**:6 (1978), 431–440.

[Gurtin et al. 1998] M. E. Gurtin, J. Weissmüller, and F. Larché, "A general theory of curved deformable interfaces in solids at equilibrium", *Philos. Mag. A* **78**:5 (1998), 1093–1109.

[Hwu 1991] C. Hwu, "Collinear cracks in anisotropic bodies", *Int. J. Fract.* **52**:4 (1991), 239–256.

[Ieşan and Scalia 2007] D. Ieşan and A. Scalia, "On the deformation of functionally graded porous elastic cylinders", *J. Elasticity* **87**:2 (2007), 147–159.

[Kim et al. 1999] S. H. Kim, K. Y. Lee, and S. C. Joo, "Stress intensity factor for orthotropic three layered material with crack under arbitrary anti-plane shear", *Theor. Appl. Fract. Mech.* **32**:2 (1999), 101–109.

[Kwon and Meguid 2002] J. H. Kwon and S. A. Meguid, "Analysis of a central crack normal to a piezoelectric-orthotropic interface", *Int. J. Solids Struct.* **39**:4 (2002), 841–860.

[Lee et al. 2002] J. S. Lee, S. M. Kwon, K. Y. Lee, and J. H. Kwon, "Anti-plane interfacial Yoffe-crack between a piezoelectric and two orthotropic layers", *Eur. J. Mech. A Solids* **21**:3 (2002), 483–492.

[Li 2003] X.-F. Li, "Closed-form solution for two collinear mode-III cracks in an orthotropic elastic strip of finite width", *Mech. Res. Commun.* **30**:4 (2003), 365–370.

[Liu and Zhou 2014] H.-T. Liu and Z.-G. Zhou, "Basic solution of a plane rectangular crack in a 3-D infinite orthotropic elastic material", *Mech. Res. Commun.* **61** (2014), 7–18.

[Liu et al. 2015] H.-T. Liu, Z.-G. Zhou, L.-Z. Wu, and W.-J. Wu, "Non-local theory solution to a rectangular crack in a 3D infinite orthotropic elastic medium", *Int. J. Solids Struct.* **58** (2015), 207–219.

[Luo and Wang 2009] J. Luo and X. Wang, "On the anti-plane shear of an elliptic nano inhomogeneity", *Eur. J. Mech. A Solids* **28**:5 (2009), 926–934.

[Moharrami and Ayatollahi 2011] A. Moharrami and M. Ayatollahi, "Anti-plane elastodynamic analysis of orthotropic planes weakened by several cracks", *Appl. Math. Model.* **35**:1 (2011), 50–60.

[Monchiet et al. 2012] V. Monchiet, C. Gruescu, O. Cazacu, and D. Kondo, "A micromechanical approach of crack-induced damage in orthotropic media: Application to a brittle matrix composite", *Eng. Fract. Mech.* **83** (2012), 40–53.

[Muskhelishvili 1953] N. I. Muskhelishvili, *Some basic problems of the mathematical theory of elasticity: Fundamental equations, plane theory of elasticity, torsion and bending*, Noordhoff, Groningen, 1953.

[Nan and Wang 2013] H. S. Nan and B. L. Wang, "Effect of crack face residual surface stress on nanoscale fracture of piezoelectric materials", *Eng. Fract. Mech.* **110** (2013), 68–80.

[Nie et al. 2008] G. H. Nie, C. K. Chan, F. G. Shin, and S. Roy, "Elliptical inhomogeneity in orthotropic composite materials due to uniform eigenstrains", *Compos. B Eng.* **39**:2 (2008), 374–385.

[Ozturk and Erdogan 1997] M. Ozturk and F. Erdogan, "Mode I crack problem in an inhomogeneous orthotropic medium", *Int. J. Eng. Sci.* **35**:9 (1997), 869–883.

[Peng et al. 2015] B. Peng, Z. Li, and M. Feng, "The mode I crack-inclusion interaction in orthotropic medium", *Eng. Fract. Mech.* **136** (2015), 185–194.

[Sharma et al. 2003] P. Sharma, S. Ganti, and N. Bhate, "Effect of surfaces on the size-dependent elastic state of nano-inhomogeneities", *Appl. Phys. Lett.* **82**:4 (2003), 535–537.

[Tang and Hwang 1991] L. Q. Tang and K. C. Hwang, "The near-tip fields for a plane stress mode I stationary crack in an elastic-perfectly orthotropic plastic material", *Acta Mech. Sinica* **23**:4 (1991), 448–457. In Chinese.

[Xiao and Jiang 2009] J. Xiao and C. Jiang, "Exact solution for orthotropic materials weakened by doubly periodic cracks of unequal size under antiplane shear", *Acta Mech. Solida Sin.* **22**:1 (2009), 53–63.

[Xiao et al. 2014] J.-h. Xiao, C.-f. Shi, Y.-l. Xu, and F.-c. Zhang, "Study on orthotropic materials containing elliptic cavity under anti-plane shear due to interface stress", *J. Yanshan Univ.* **38**:3 (2014), 272–276. In Chinese.

[Yang and Becker 2004] Q.-S. Yang and W. Becker, "Effective stiffness and microscopic deformation of an orthotropic plate containing arbitrary holes", *Comput. Struct.* **82**:27 (2004), 2301–2307.

[Zhang and Deng 2008] W. Zhang and X. Deng, "Asymptotic stress field in a degenerate orthotropic material containing a cohesive zone ahead of a crack tip", *J. Elasticity* **90**:3 (2008), 271–282.

[Zhao and Yu 2000] A. Zhao and J. Yu, "The overall elastic moduli of orthotropic composite and description of orthotropic damage of materials", *Int. J. Solids Struct.* **37**:45 (2000), 6755–6771.

Received 6 Jul 2015. Revised 17 Mar 2016. Accepted 22 Mar 2016.

JUNHUA XIAO: xiaojunhua@ysu.edu.cn
*Key Laboratory of Mechanical Reliability for Heavy Equipments and Large Structures of Hebei Province, Yanshan University, Qinhuangdao, 066004, China*

CHUANFU SHI: 794509661@qq.com
*Key Laboratory of Mechanical Reliability for Heavy Equipments and Large Structures of Hebei Province, Yanshan University, Qinhuangdao, 066004, China*

YAOLING XU: xylysu@163.com
*Key Laboratory of Mechanical Reliability for Heavy Equipments and Large Structures of Hebei Province, Yanshan University, Qinhuangdao, 066004, China*

FUCHENG ZHANG: zfc@ysu.edu.cn
*State Key Laboratory of Metastable Materials Science and Technology, Yanshan University, Qinhuangdao, 066004, China*

# JOURNAL OF MECHANICS OF MATERIALS AND STRUCTURES

msp.org/jomms

Founded by Charles R. Steele and Marie-Louise Steele





Cover photo: Wikimedia Commons

See msp.org/jomms for submission guidelines.

JoMMS (ISSN 1559-3959) at Mathematical Sciences Publishers, 798 Evans Hall #6840, c/o University of California, Berkeley, CA 94720-3840, is published in 10 issues a year. The subscription price for 2016 is US $575/year for the electronic version, and $735/year (+$60, if shipping outside the US) for print and electronic. Subscriptions, requests for back issues, and changes of address should be sent to MSP.

JoMMS peer-review and production is managed by EditFlow® from Mathematical Sciences Publishers.

PUBLISHED BY

mathematical sciences publishers

nonprofit scientific publishing

http://msp.org/

# Journal of Mechanics of Materials and Structures

Volume 11, No. 5 December 2016